

Band-gap renormalization in modulation-doped $\text{In}_{1-x}\text{Ga}_x\text{As}/\text{GaAs}$ V-shaped quantum wires

R. Rinaldi, G. Coli', A. Passaseo, and R. Cingolani

*Istituto Nazionale di Fisica della Materia-Unità di Lecce, Dipartimento di Scienza dei Materiali,
Università degli Studi di Lecce, via Arnesano, 73100 Lecce, Italy*

(Received 11 March 1998)

We have investigated the quasi-one-dimensional electron plasma confined in modulation doping $\text{In}_{1-x}\text{Ga}_x\text{As}/\text{GaAs}$ V-shaped quantum wires. The band-gap renormalization is extracted from the optical spectra and compared to a suitably developed theoretical model. We find that band-gap renormalization is reduced in one-dimensional systems as compared to quantum wells. [S0163-1829(98)00543-8]

I. INTRODUCTION

Recently there has been increasing interest in the problem of many-body effects and band-gap renormalization in one-dimensional structures.¹⁻⁶ Most of the experimental results¹⁻⁵ point towards a band-gap renormalization smaller than in quantum wells at any carrier density. The lack of strong band-gap renormalization also raises the interesting question about the excitonic character of the spontaneous and stimulated emission in quantum wires. On the other hand, previous theories developed for many-body effects in quasi-one-dimensional structures predict rather large band-gap shrinkage,^{7,8} and clearly show many-body-induced exciton screening at high density.⁶ Even though there is a general consensus about the reduction of band-gap renormalization (BGR) in low-dimensional systems, the quantitative assessment of the density dependence of the BGR in quantum wires is still a subject of debate.

In this paper, we present the quantitative determination of band-gap renormalization in modulation doping V-shaped $\text{In}_{1-x}\text{Ga}_x\text{As}/\text{GaAs}$ quantum wires. The careful control of the n -type plasma density confined in the ground state of the wire is exploited to investigate the changes of the optical properties of the nanostructure induced by many-body effects. The density dependence of the band-gap renormalization is obtained from the analysis of the optical spectra, exploiting the exact knowledge of the doping density introduced by the growth, and is compared to a purposely developed theoretical model, based on the random-phase approximation. The comparison between theory and experiments clearly indicates that band-gap renormalization for the electron plasma does not exceed 10 meV for carrier densities of the order of 10^6 cm^{-3} , consistent with the qualitative indications recently reported in the literature³⁻⁵ in narrow wires. Both the absolute values and the density dependence of the BGR of the quantum wires are thus found to be smaller than in quantum wells.

II. EXPERIMENT

The V-shaped quantum wires were grown by metal-organic chemical-vapor deposition on patterned GaAs substrates. The patterned substrates were fabricated by holographic photolithography and wet-chemical etching. The grown structures consist of 50-nm GaAs buffer layer, 20-nm

Si-doped GaAs, 6-nm GaAs space layer, a single 3-nm (nominal width) $\text{In}_{0.1}\text{Ga}_{0.9}\text{As}$ well, 6-nm GaAs space layer, 20-nm Si-doped GaAs, and 30-nm GaAs cap layer. Details on the growth can be found in Ref. 9. Three samples with the same structure and different doping density were grown: sample *A* with $3 \times 10^{18}/\text{cm}^3$; sample *B* with $6 \times 10^{17}/\text{cm}^3$; and sample *C* with $7 \times 10^{16}/\text{cm}^3$. An undoped structure with similar layer sequence was also grown as a reference. The unpatterned region of the samples was used to measure the spectra of the planar quantum wells, in order to compare the quantum-well and quantum-wire BGR fabricated under identical growth and doping conditions.

The photoluminescence and excitation photoluminescence experiments were performed by using a Ti:sapphire laser as exciting source. The emitted light was dispersed and detected by a double 0.85-m monochromator equipped with a photon counting acquisition module.

III. RESULTS

The 10-K photoluminescence (PL) and excitation photoluminescence (PLE) spectra of the modulation doping wires are shown in Fig. 1. All the measured PL spectra show the emission band of the quantum-wire plasma around 1.47 eV, the GaAs barrier emission around 1.518 eV, and a carbon related transition around 1.494 eV. With increasing plasma density, the quantum-wire emission band redshifts, broadens, and loses intensity. The many-body effects on the absorption profile of the wires are clearly seen in the PLE spectra of Fig. 1. The PLE spectrum of sample *C* shows two well-resolved resonances around 1.474 and 1.489 eV, which are ascribed to the $n_y=1$ and $n_y=2$ levels in the wire. At intermediate plasma density, the PLE spectrum of sample *B* exhibits a partially bleached absorption edge shifted to higher energy with respect to sample *C*. In this case, the $n_y=1$ state is partially filled, and a Burstein-Moss shift of the order of 10 meV is seen between PL and PLE. At the highest density ($3 \times 10^{18} \text{ cm}^{-3}$, corresponding to approximately $1 \times 10^6 \text{ cm}^{-1}$ in the wire) the conduction-band states are filled, and the Fermi edge lies close to the edge of the quantum-wire barrier. Under this condition, the quantum-wire absorption is totally bleached, up to about 1.5 eV, and the Burstein-Moss shift exceeds 25 meV. We also note a general degradation of the PLE profile, which is affected by

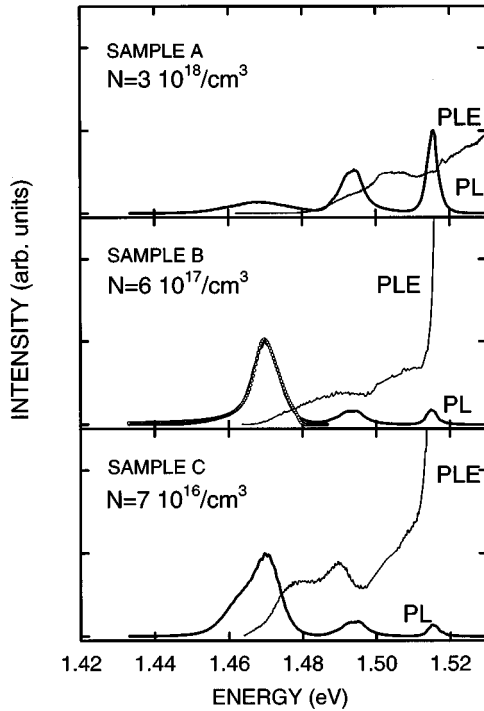


FIG. 1. PL (thick solid lines) and PLE (thin solid lines) spectra of the modulation-doping quantum-wire samples at 10 K. The power density is 10 W/cm^2 . The low-energy shoulder of the PL spectrum of sample C is due to impurity related transitions and readily disappears with increasing the excitation intensity.

a strong broadening even at the barrier edges, probably due to impurity interdiffusion.

In order to get quantitative information on the plasma parameters we have fitted the PL line shape $[L(\hbar\omega)]$ of the modulation doping wires and of their reference quantum wells by the usual statistical recombination model,^{1-3,10,11} $L(\hbar\omega) \approx g(\hbar\omega, \Gamma) f_e(\hbar\omega) f_h(\hbar\omega)$, where partial lifting of k conservation is accounted for by a Gaussian convolution of the one- and two-dimensional joint density of states $g(\hbar\omega, \Gamma)$ for the quantum wires and quantum wells, respectively. The typical broadening parameter Γ was found to be in the range of 3–4 meV for all samples. f_e and f_h are the Fermi distribution functions for the electrons and holes, respectively. The main advantages of using modulation doping structures are that the carrier density is known from the doping density with good accuracy¹² and the electron plasma is thermalized at the crystal temperature. This reduces the number of free parameters adopted in the line-shape fitting of the PL spectra, and minimizes the artifacts of the fitting procedure. In particular, our line-shape fitting was performed assuming a carrier temperature (T_c) of the order of 1 meV, because of the extremely low cw excitation power used in the experiments, which ensures that T_c is of the same order of the lattice temperature ($T_c \approx 10 \text{ K}$). Correspondingly, the quasi-Fermi level of the electrons was calculated according to the usual zero-temperature expressions, $F_e^{2D} = (\pi\hbar^2/m_e)N^{2D}$ and $F_e^{1D} = (\hbar^2\pi^2/8m_e)(N^{1D})^2$ for the two-dimensional and one-dimensional electron plasma, respectively, taking the nominal doping density N scaled in one- and two-dimensional units. The hole Fermi level was assumed to be zero, because the photoinjected hole density is supposed to be negligible

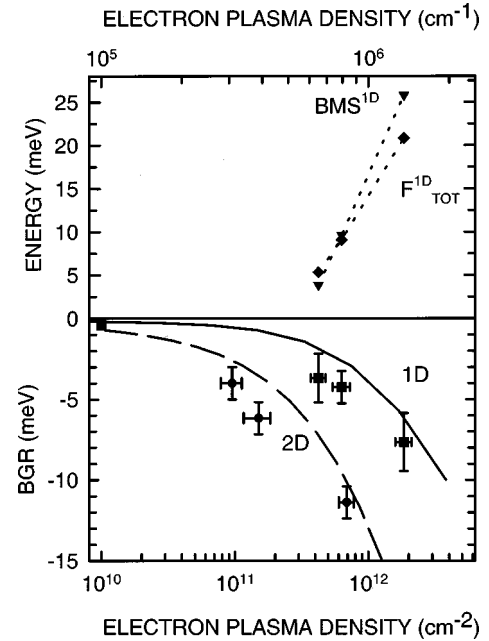


FIG. 2. Band-gap renormalization (BGR) of quantum wires (1D, squares) and quantum wells (2D, dots), Burnstein-Moss shift of the wires (BMS^{1D}, downward triangles), and Fermi energy of the wires (F_{tot} , diamonds) as a function of the electron plasma density. The continuous and dashed lines represent the BGR calculated according to our theoretical model for quantum wires and quantum wells, respectively (see text). The dotted lines are guides for the eye.

with respect to the pre-existing electron-density.

With these important parameters fixed, the line-shape analysis becomes a simple fitting procedure in which the BGR is the only physical free parameter (besides the amplitude parameter, which does not bring any physical information and is used to match the intensity of the calculated and measured spectra). The dotted line in Fig. 1 represents the best fit to one of the PL spectra, which describes quite reasonably the optical spectra by using the nominal density parameters.¹³ As expected, the energy position of the renormalized band gap falls in the low-energy tail of the luminescence band.¹ PL spectra measured up to 80 K were also analyzed, showing similar results. Beyond this temperature the emission was dramatically reduced due to thermal escape of carriers outside the wire.

In Fig. 2 we plot the one-dimensional (1D, squares) and two-dimensional (2D, dots) BGR values versus the plasma density. The band-gap renormalization was obtained by comparison with the $n_y=1$ state of the undoped sample. The Burnstein-Moss shift evaluated by the difference between the renormalized band-gap edge and the edge of the PLE curve¹⁴ (downward triangles in Fig. 2) is consistent with zero-temperature one-dimensional Fermi energies obtained by the nominal carrier density values [$k_F(N) = \pi N^{1D}/2$] (diamonds in Fig. 2), with an indetermination of the order of 10%. This indetermination is indicated by the horizontal error bars in the BGR of Fig. 2. The vertical error bars in the BGR values represent the best-fit accuracy in the band-gap determination.

A band-gap renormalization of a few meV is observed under our experimental conditions. The measured BGR values are smaller than those observed in the quantum well. At

the highest plasma density ($1.1 \times 10^6 \text{ cm}^{-3}$) the quantum-wire BGR amounts to 7.65 meV, which puts an upper limit of about 15 meV for the neutral electron-hole plasma of density of the order of 10^{18} cm^{-3} in the wires. This should be compared to about 25 meV for an e - h plasma confined in the corresponding quantum wells at comparable density. These experimental data indicate that BGR is reduced in the wires with respect to the reference quantum wells. This is in agreement with the early results reported in Ref. 2, where the quantum-wire BGR, extracted by a multiparameter line-shape fitting procedure, was smaller than the BGR found in the reference quantum well. In that case however, the wires had still some two-dimensional character (rectangular wires of lateral width $\sim 55 \text{ nm}$) and the measured BGR was close to the 2D limit (around 20 meV at high density).

IV. DISCUSSION

In order to quantitatively analyze these data we have calculated BGR in our V-shaped modulation doping quantum wires and in the reference modulation doping quantum wells. For that purpose, we have developed a multidimensional theoretical model that describes the BGR for systems of arbitrary dimensionality. In our model, we describe the many-body interactions in the frame of random-phase approximation (RPA). The correction to the eigenenergies (self-energy Σ) is obtained by adding the ring-diagram contribution to the correlation energy, and the exchange term at first order, i.e.,

$$\Sigma(\vec{k}, \omega) = \Sigma_{\vec{q}} \int \frac{d\alpha}{2\pi} \frac{V(|\vec{q}|)}{1 - \Pi(\vec{q}, \alpha)V(|\vec{q}|)} G(\vec{k} - \vec{q}, \omega - \alpha), \quad (1)$$

where $V(\vec{q})$ is the matrix element of the bare Coulomb interaction, $G(\vec{k}, \alpha)$ is the Green's propagator, and $\Pi(\vec{q}, \alpha)$ is the longitudinal polarizability function of semiconductors. We have obtained an analytical expression for the longitudinal polarizability $\Pi(\vec{q}, \alpha)$ in the frame of the RPA:

$$\Pi(\vec{q}, \alpha) = n_p(1 - n_{p+\vec{q}})|_{p_0^-} d(\hbar\alpha - E_q + i\delta) - n_p(1 - n_{p+\vec{q}})|_{p_0^+} d(\hbar\alpha + E_q + i\delta), \quad (2)$$

where $\hbar\alpha$, $E_q = \hbar^2 q^2 / 2m$, and n_q are the energy parameter, the exchanged kinetic energy, and the Fermi-Dirac distribution of the quasiparticle, respectively; whereas $p_0^\pm = \sqrt{(m/\hbar^2)|\hbar\alpha \pm E_q + i\delta|}$, δ is a damping factor. The spectral-density function results:

$$d(\hbar\alpha \pm E_q + i\delta) = -i C_{\text{dim}} \left(\sqrt{\frac{2m}{\hbar^2}} \right)^{\text{dim}} \frac{|\sqrt{\hbar\alpha \pm E_q + i\delta}|^{\text{dim}-1}}{\sqrt{\hbar\alpha \pm E_q + i\delta}}, \quad (3)$$

where dim indicates the dimensionality of the heterostructure, C_{dim} is a constant and is $1/\pi$ for quantum wells, and $2/\pi$ for quantum wires. In order to evaluate Eq. (1), we adopt the static limit of the single plasmon-pole approximation:

$$\frac{1}{\epsilon(q, N)} = \frac{1}{1 - \Pi(\vec{q}, N)V(\vec{q})} = 1 - \frac{\omega_{pl}^2(q, N)}{\omega_q^2(q, N)}. \quad (4)$$

The plasmon frequency is given by

$$\omega_q^2(N) = \omega_{pl}^2(q, N)[1 + a_B/\tilde{\lambda}(q, N)] + C(q)E_q^2, \quad (5)$$

where $C(q) = \Delta_{\text{dim}} q^{\text{dim}} V^{\text{eff}}(q) / (\hbar^2 R_y)$, $\Delta_{\text{dim}} = 1/4\pi$ in three dimensions, $\Delta_{\text{dim}} = 1/2\pi$ in two dimensions, and $\Delta_{\text{dim}} = 1$ in one dimension, $a_B = \hbar^2 \epsilon_0 / m e^2$, $R_y = m e^4 / 2 \hbar^2 \epsilon_0^2$, and

$$\begin{aligned} \tilde{\lambda}(q, N) &= \frac{\epsilon_0}{e^2} \Delta_{\text{dim}} V^{\text{eff}}(q) \tilde{k}(N) \frac{1}{\sqrt{2}} \\ &\times [q^4 + (\delta/c^2)^2]^{(\text{dim}-2)/4} \sqrt{1 + \frac{q^2}{\sqrt{q^4 + (\delta/c^2)^2}}}, \\ \tilde{k}(N) &= 2(1 - \exp\{-\hbar^2[k_F(N)]^2/2m\}). \end{aligned}$$

The plasma frequency is

$$\omega_{pl}^2(q, N) = [k_F(N)]^{\text{dim}} \Delta_{\text{dim}} q^2 V^{\text{eff}}(q) / m. \quad (6)$$

In Eq. (6), $1/\beta = K_B T$ is the thermal energy of the particles, $k_F(N)$ is the self-consistent Fermi wave vector as a function of the carrier density (N) and thermal energy. Our treatment does not depend on the effective expression for the bare Coulomb matrix element, and for the case of a one-dimensional plasma we adopt the simplest hypothesis of separable confinement in a quantum wire, and we choose a square-well confinement along the growth direction (x) and parabolic confinement along the lateral y direction. The expression of the bare Coulomb matrix element turns out to be

$$V^{\text{eff}}(q) = \frac{2e^2}{\epsilon_0} \frac{1}{\Omega_{1D}} \int_0^{L_x} \int_0^{L_y} K_0(q\sqrt{x^2 + y^2}) f(x) g(y) dy dx, \quad (7)$$

where

$$\begin{aligned} f(x) &= \left[\frac{\sqrt{\pi}}{\alpha} \Phi(\alpha L_x / 2) \right]^{-2} \frac{\sqrt{\pi/2}}{\alpha} \Phi[\alpha(L_x - x)/\sqrt{2}] \\ &\times \exp(-\alpha^2 x^2 / 2), \\ g(x) &= \frac{1}{L_y} \left\{ \left(1 - \frac{y}{L_y} \right) \left[2 + \cos\left(\frac{2\pi y}{L_y} \right) \right] + \frac{3}{2\pi} \sin\left(\frac{2\pi y}{L_y} \right) \right\}. \end{aligned} \quad (8)$$

$\Phi(x)$ is the probability integral and $K_0(x)$ is the modified, zero-order Bessel's function. L_x and L_y are the confinement lengths of the wire, $\alpha = \sqrt{E_0} 2m/\hbar^2$ and E_0 is the ground level of the wire. The corresponding expressions for the effective Coulomb matrix element in quantum wells can be found in the literature.¹⁵

The calculated BGR values are displayed in Fig. 2 by the continuous line for the quantum wires and by the dashed line for the quantum wells. The theory predicts relatively small BGR values for the wires, in agreement with our experimental values and consistent with the qualitative indications of recent reports.³⁻⁵ The theoretical 1D BGR values are smaller than those reported by previous theoretical works.^{7,8} This is probably due to the realistic expression for the longitudinal

dielectric function developed in our work, which gives less divergent contribution to the screened scattering matrix element in the calculation of the self-energy. This is important for the description of the interband processes in an electron-hole plasma, where many-body interactions take place through a Coulomb potential dressed by many-particle interactions of electrons and holes in their bands. In this case, a fully screened potential implies a small contribution of correlated pairs to the many-body nonlinearity. We should mention that the small discrepancy between the experimental data and the theoretical prediction in Fig. 2 can be reduced by using exact wave functions calculated for the specific quantum-wire heterostructure, by evaluating numerically Eqs. (2) and (3), and by using a more advanced PL line-shape fitting model. Nonetheless, the agreement between theory and experiments is very satisfactory, both for the absolute BGR values and for its density dependence, clearly demonstrating that the one-dimensional confinement reduces BGR. Also in the case of our quantum wells, the agreement between the theoretical data and the experimental values is

quite good. Our data indicate that for plasma densities higher than 10^{12} cm^{-2} the BGR of the one-component plasma is of the order of 15 meV, that is, roughly twice the value found for the wires under the same experimental conditions.

In conclusion, we have fabricated n -type modulation-doping $\text{In}_{1-x}\text{Ga}_x\text{As}/\text{GaAs}$ V-shaped quantum wires. The band-gap renormalization has been extracted from the optical spectra and compared to a specific model developed in the frame of RPA. The resulting picture of many-body effects in quantum wires is consistent with the existence of a small but observable BGR (about 7 meV for an electron plasma of densities $\approx 10^6/\text{cm}^2$).

ACKNOWLEDGMENTS

The expert technical help of A. Melcarne, A. Miccolis, and D. Cannoletta is gratefully acknowledged. This work was supported by the INFM Progetto Sud: "V-shaped quantum wires for optoelectronic applications."

¹R. Cingolani, R. Rinaldi, M. Ferrara, G. C. LaRocca, H. Lage, D. Heitmann, K. Ploog, and H. Kalt, *Phys. Rev. B* **48**, 14 331 (1993).

²R. Cingolani, R. Rinaldi, M. Ferrara, G. C. LaRocca, H. Lage, D. Heitmann, and H. Kalt, *Semicond. Sci. Technol.* **9**, 875 (1994).

³M. Grundmann, J. Christen, M. Joschko, O. Stier, D. Bimberg, and E. Kapon, *Semicond. Sci. Technol.* **9**, 1939 (1994).

⁴W. Wegscheider, L. N. Pfeiffer, M. M. Dignam, A. Pinczuk, K. W. West, S. L. McCall, and R. Hull, *Phys. Rev. Lett.* **71**, 4071 (1993).

⁵R. Ambigapathy, I. Bar-Joseph, D. Y. Oberli, S. Haacke, M. J. Brasil, F. Reinhardt, E. Kapon, and B. Deveaud, *Phys. Rev. Lett.* **78**, 3579 (1997).

⁶F. Rossi and E. Molinari, *Phys. Rev. Lett.* **76**, 3642 (1996).

⁷S. Benner and H. Haug, *Europhys. Lett.* **16**, 579 (1991).

⁸Ben Yu-Kuang Hu and S. Das Sarma, *Phys. Rev. B* **48**, 5469 (1993).

⁹R. Rinaldi, A. Passaseo, M. DeGiorgi, C. Turco, M. DeVittorio, D. Cannoletta, and R. Cingolani, *Solid-State Electron.* **42**, 1239 (1998).

¹⁰G. Lasher and F. Stern, *Phys. Rev.* **133**, A553 (1964).

¹¹J. Christen and D. Bimberg, *Phys. Rev. B* **42**, 7213 (1990).

¹²Y. Zhang, R. Cingolani, and K. Ploog, *Phys. Rev. B* **44**, 5958 (1991).

¹³It is worth noting that we have also tried to fit the line shapes by using all the parameters free, including quasi-Fermi levels and temperature. In this case, convergency was obtained with temperatures in the range of 1–2 meV and densities very close to the doping density (within 10%), with similar BGR values.

¹⁴The edge of the PLE spectra was taken at half maximum of the absorption edge.

¹⁵I. Galbraith, P. Dawson, and C. T. Foxon, *Phys. Rev. B* **45**, 13 499 (1992).